academicJournals

Vol. 8(2), pp. 13-27, July, 2016
DOI: 10.5897/JGMR2015.0230
Article Number: 9FB684759542
ISSN 2006-9766

http://www.academicjournals.org/JGMR

Journal of Geology and Mining Research

Full Length Research Paper

Highlighting the root of a paleoproterozoic oceanic arc in Liptako, Niger, West Africa

Soumaila Amadou[1], Garba Zibo[1,3], Moussa Issaka Abdoulkader[2]*, Nouhou Halitt[1] and Sebag David[4,5,6]

[1]Department of Geology, University of Abdou Moumouni, Niamey, Niger.
[2]Department of Geological and Environmental Sciences, University of Zinder, Niger.
[3]University of Dosso, Niger.
[4]University of Rouen, CNRS, Mont-Saint-Aignan, France.
[5]HydroSciences of Montpellier, IRD, France.
[6]Université de Ngaoundéré, Cameroun.

Received 5 July, 2015; Accepted 25 May, 2016

In the southwest branch of the Diagorou-Darbani greenstone belt, mafic to ultramafic plutonic rocks outcrop in Pogwa area. Field relations show that these rocks are clearly intrusive in flattened pillowed-metabasaltes. They are made up of gabbros and pyroxenites with ultramafic rocks cropping out as panels or scattered lenses. Petrographic characters are suggestive of metamorphic grade varying from greenschist to amphibolite facies. The geochemical characters revealed that most of the gabbroic rocks were generated by fractional crystallization; however, variations in Ni and Cr contents in some samples are attributed to variable degrees of partial melting. The rare earth elements REE and spider diagrams distinguished two kinds of patterns: 1) most rocks with light rare earth elements LREE enriched patterns, heavy REE HREE depleted patterns, large ion lithophile elements LILE enrichment and negative anomalies in high field strength elements HFSE (Nb, Ta, Zr and Hf). These features are suggestive of an oceanic arc emplacement, corroborated by Zr-Nb-Y and Cr-Y discrimination diagrams. 2) The other (Ultramafic rocks and metatonalite) with tholeiitic character with REE patterns depleted in LREE and enriched in HREE. In fact, the tonalite rock may represent a highly evolved term of an ultramafic-mafic suite of oceanic crust. The mafic and ultramafic rocks of Pogwa constituted the out cropping root of a paleoproterozoic oceanic-arc in the birimian formations in Liptako, Niger.

Key words: Liptako, Pogwa, palaeaoproterozoic, oceanic arc, root.

INTRODUCTION

Precambrian rocks of the West African craton outcrop in two shields: the Reguibat shield in the northern part and the Man or Baoulé-Mossi shield in the southern part (Figure 1A). The Archean rocks are exposed in the western parts of these shields, while the paleoproterozoic ones (birimians rocks) constitute the basement of the eastern zones. The Birimian formations are characterized by an alternating granitoids and linear or curved have

*Corresponding author. E-mail: Kader_geol@yahoo.fr. Tel: (00227)99322286.

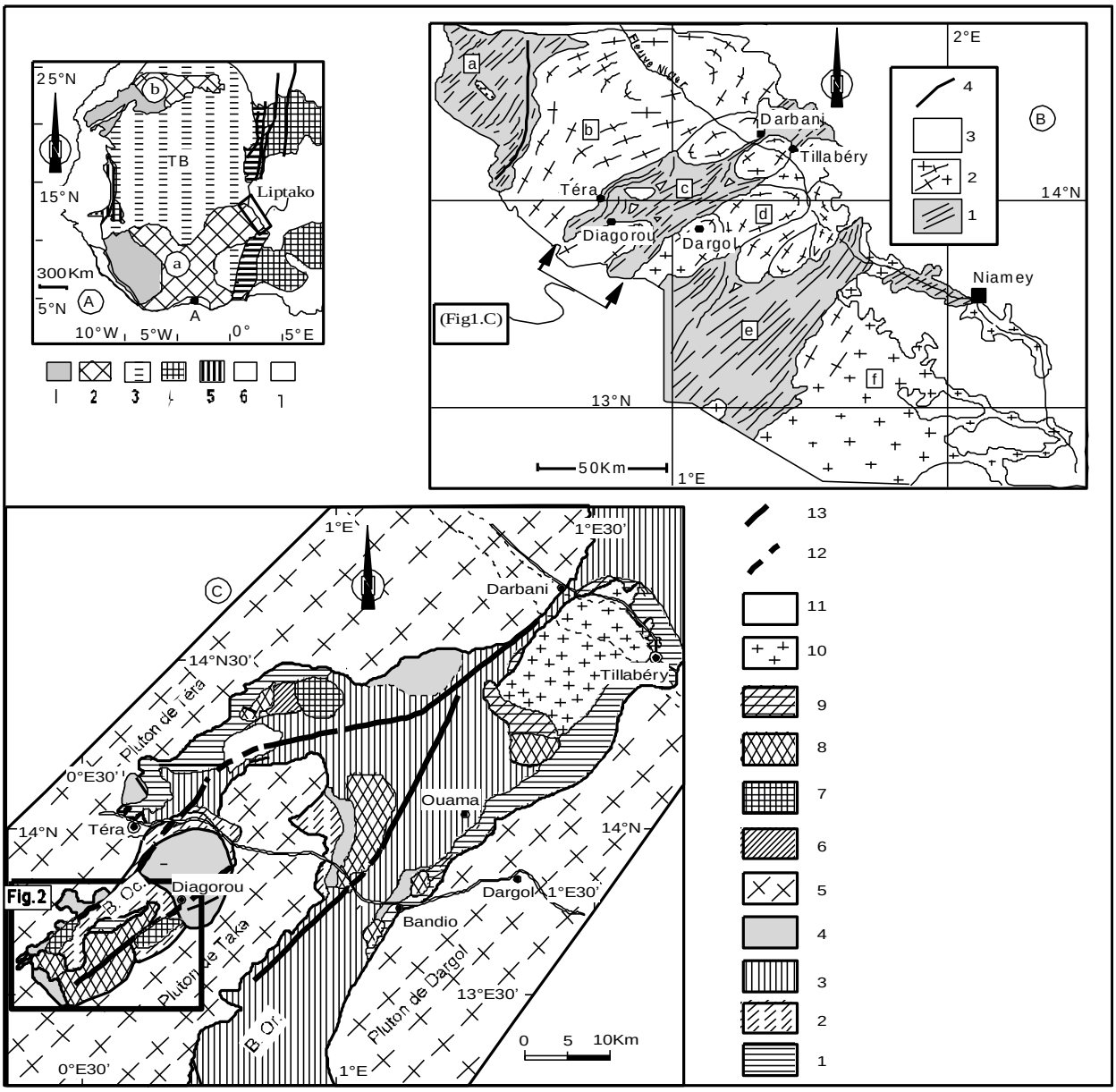

Figure 1. A) Geographical map of the West African Craton and PanAfrican reworked zones. a) Man shield, b) reguibat shield, TB: Touareg shield, 1: Archean rocks; 2: Birimian rocks; 3: Precambrian basins; 4: reworked basement; 5: reworked zones; 6: Phanerozoic basins. B) Geographical map of Liptako (Dupus et al., 1990). 1: Greenstone salts; 2: granitold plutons; 3: sedimentary cover; 4: tectonic contact; a: Goroul greenstone belt; b: Tera pluton; c: Diagorou-Darbani greenstone belt; B: Occ Westren branch; B. Or Eastern Branch; d: Dargol pluton; e: Sirba greenstone belt; f: Torodi Pluton. C) Geological map of the Diagorou-Darbani greenstone belt. 1: Metabaslats; 2: Talcschists and Talc-chloritoschist, 3: Metasediments and volcano-sediments; 4: Amphibphites with locally associated micaschists; 5: Granitoids; 6: Gabbros; 7: assemblages of basic and ultrabasic rocks; 8: Quartz Metadiorites; 9: Calc-alcalines volcanic rocks; 10: Late granits; 11: Syenithic rock; 12: Uncertain shearzone; 13: Shear zone.

witnessed a period of major crustal accretion from greenstone belts. In West Africa, they are considered to 2.1 Ga (Abouchami et al., 1990; Boher et al., 1992) to 2.3 Ga (Lahondère et al., 2002; Gasquet et al., 2003; Soumaila et al., 2008). The greenstone belts are made up of mafic rocks (volcanic and plutonic), sedimentary and/or volcano-sedimentary rocks. They are generally metamorphosed in low greenschist locally, amphibolit facies conditions, especially in greenstone belts - granitoid contacts (Dupuis et al., 1991; Pons et al., 1995; Soumaila et al., 2006).

The mafic rocks are of tholeiitic composition,

suggesting that they are emplaced in geodynamic context similar to that of oceanic plateau in Ivory Cost (Abouchami et al., 1990), or to that of oceanic arc context in Niger (Ama-Salah et al., 1996; Pouclet et al., 1996). More complex geodynamic environments, with interaction between mantle plumes and subduction zones with associated back-arc basins have been suggested (Soumaila et al., 2004).

The compilation of chemical data from greenstone belts of the whole West African craton suggested that large volcanic basic rocks were produced by a mantle plume in oceanic domain. This volcanic event was followed by a subsidence related to plateau basalts weight. Partial melting took place at the bottom of the mafic pile, with production and rising of granitoid melts (Lompo, 2009).

Locally, in Niger and Burkina Faso, assemblages of ultramafic to mafic plutonites crop out in the greenstone belts. In Burkina Faso, these assemblages have been suggested to be relics of magmatic chamber at the base of oceanic arc (Beziat et al., 2000). In Niger, such ultramafic to mafic plutonic rocks out crop in the Pogwa sector in Diagorou-Darbani greenstone belt (Machens, 1973), but they are poorly studied. This paper aims at studying the petrographic and geochemical features of these rocks in order to highlight their character and geodynamic emplacement.

Regional geology

In Niger, birimian rocks crop out in the Liptako area, the northeastern most part of Man shield. The geological feature of this area is greenstone belts alternating with granitoid plutons (Figure 1A). From northwest to southeast greenstone belts are of Gorouol, Diagourou-Darbani and Sirba. The granitoid plutons are of Tera, Dargol and Torodi (Figure 1B). Westward, the Diagorou-Darbani greenstone is flanked by the Tera pluton, and eastward the Dargol one. Geochronologic ages of these granitoid plutons range from 2.15 to 2.18 Ga (Cheilletz et al., 1994; Amah-Salah, 1996; Soumaila et al., 2008). Both greenstone belts of Diagorou - Darbanis are composed of metabasalts distorted into talcschistes and chloritoschistes and also contain locally mafic plutonic to ultramafic rocks. Garnet and garnet-free-amphibolites, kyanite – staurolite – garnet - micaschistes, quartzites, garnet-quartzites, and grenatites occurred near the contact with Tera pluton. Sediments and volcano-sediments, weakly metamorphosed in the greenschist facies and crop out largely in the northeastern and eastern part of the green stone belt. In the halt southern most part, the Diagorou-Darbani greenstone belt is divided into two branches by the Taka pluton: a western branch dominantly composed of metamagmatic rocks and the eastern branch mainly made up of meta-sediments and metavolcano-sediments rocks. Small granitic and dioritic stocks, associated locally with volcanic rocks, cross cut the latter. The sector of Pogwa is the southwestern most part of the Diagorou-Darbani greenstone belt, where mafic to ultramafic plutonites are intrusive in metabasaltes and talcshistes.

MATERIALS AND METHODS

Aerial photographs have been selected to cover the sector of Pogwa in order to draw a detailed geological map. Tree Cross-sections (A, B, and C) are carried out to establish chronologic succession of formations. Two field missions, with sampling surveys, have been undertaken. About fifty samples were collected, and seventeen samples were selected for thin sections to perform petrographic studies. Thin sections were prepared in the laboratory at the Department of Geology, University of Abdou Moumouni. Geochemical analyses on the total of the rocks were performed by the Rocks and Material Analysis Service of Petrographic and Geochemical Research Center Nancy, France. Major elements (Si, Al, Ti, Mg, Fe, Mn, Ca, Na, K, P) were measured by atomic emission spectrometer (inductively coupled plasma Atomic Emission Spectrometer-ICPAES). Samples were crushed and brought to fusion with Li_2BO_2 and dissolved in 2% HNO_3.The sample solution is introduced into the emission spectrometer (Thermo Fischer ICap 6500). It becomes atomized with argon gas into hot plasma. The outer-shell electrons of the elements in the sample are excited, emitting light wavelengths which is an energy characteristic of its elements. A mirror reflects the light through the entrance of the spectrometer which separates particular element wavelengths and directing each of them to a specific photomultiplier tube detector. The more intense this light is, the more concentrated the element. A computer converts the electronic signal from the photomultiplier tubes into concentrations. The limits of detection are of 0 2% for SiO_2, Al_2O_3 0.1%, Fe_2O_3, MgO. The mass spectrometer (ICP-MS) Agilent 7700X was used to measure trace elements concentrations. The sample solution is introduced into ionizing where it is atomized with argon gas into hot plasma. Four electrically charged rods (the quadruple mass filter) separate appropriate ions according to the ratio m/z (m = mass of element and z = charge). These ions arrive at the detector for counting. Electrical signals received at the detector are amplified, processed by a computing system, and converted into concentrations of elements.Trace elements were measured with the detection limits of 2 ppm (Ba), 1.5 ppm (Pb, V) 1ppm (Sb), 4ppm (Cu) 5ppm (Cr), 6ppm (Ni) 8ppm (Zn) and 0.1 to 0.005 ppm for the other trace elements and REE (Table 1).

RESULTS

Map and cross-sections

Geological map (Figure 2) shows rocks cropping out in the Pogwa-Ladanka sector. The sector is made up of amphibolites and metabasaltes, assemblages of mafic to ultramafic plutonic rocks, talcschistes, quartz-diorite, late- to post tectonic granites and decametric to multi-decametric dykes of quartz trending NE-SW and cross cutting the others. Field relationships revealed that the protolith of the talcschistes clearly has a post date of amphibolites and metabasaltes. The mafic to ultramafic plutonic rocks were weakly deformed in greenschist facies and seem intrusive in talcschistes. The relations

Table 1: Majors and trace elements analyses of the Pogwa Rocks

Samples	Fpd-21	Fpd-21	Fpd-3	Fpd-22	Fpd-4	Fpd-5	Fpd-13	Fpd-7	Fpd-17	Fpd-18	Fpd-20	Fpd-12	Th738	Th538	Fpd-9	Fpd-10
Name	**Metapyrox.**			**Metagabbro**			**Grt-A**		**Grt free A**			**F-Amp**	**Ultrabasic R.**		**Q-Dio**	**Tonal.**
SiO_2	49.36	50.42	45.45	46.46	44.57	49.39	43.66	44.79	45.38	44.54	45.63	55.52	39.63	44.46	60.29	68.52
Al_2O_3	7.81	6.63	19.45	20.45	23.06	26.40	21.95	24.18	23.48	17.62	23.31	9.50	3.14	5.78	15.56	15.55
Fe_2O_3	1.31	1.34	1.02	1.02	0.79	0.45	1.28	0.92	0.92	1.28	0.94	0.97	1.25	0.98	0.33	0.48
FeO	11.74	12.03	9.16	9.17	7.09	4.09	11.51	8.22	8.24	11.48	8.42	8.68	11.27	8.78	5.62	4.31
MnO	0.21	0.24	0.13	0.12	0.08	0.06	0.17	0.10	0.10	0.16	0.11	0.18	0.18	0.15	0.09	0.15
MgO	14.35	14.66	7.67	5.97	5.13	2.05	4.69	4.49	4.47	8.77	4.95	11.70	32.19	29.50	4.48	1.07
CaO	12.06	12.12	11.72	11.88	12.53	13.15	12.33	13.59	13.41	12.11	13.19	11.05	2.57	4.23	6.76	5.79
Na_2O	0.81	0.76	2.00	2.40	2.12	2.57	2.04	2.08	2.00	1.62	2.04	1.37	0.19	0.05	3.78	3.01
K_2O	<L.D.	<L.D.	0.51	0.11	1.07	<L.D.	<L.D.	<L.D.	<L.D.	0.13	0.05	0.09	0.00	0.00	0.87	0.07
TiO_2	0.65	0.46	0.55	0.87	0.58	0.37	1.47	0.72	0.76	1.15	0.77	0.32	0.09	0.14	0.48	0.34
P_2O_5	0.06	0.09	0.06	0.16	0.09	0.16	0.25	0.16	0.12	0.05	0.08	0.05	0.07	0.05	0.20	0.13
PF	1.22	1.12	2.23	1.24	2.76	1.14	0.54	0.56	0.90	0.94	0.60	0.98	8.40	5.31	0.08	0 .41
Total	98.58	99.87	98.93	99.85	99.87	99.83	99.89	99.81	99.68	99.85	100.1	100.4	98.99	99.43	99.89	99.83
Ba	33.26	22.24	139.90	77.25	449.60	112.40	128.00	54.61	86.36	74.21	72.98	138.70	9.50	0 ;90	434.00	151 .40
Ce	18.56	22.60	8.50	21.76	8.76	18.48	22.19	15.27	14.80	16.09	14.97	14.86	1.04	0.66	37.10	14.00
Co	53.98	58.51	39.78	36.59	35.56	12.40	33.78	29.36	27.68	54.91	30.39	47.09	117.00	83.90	23.80	5.00
Cr	1499	743.70	198.90	154.10	198.90	154.10	19.16	49.09	9.94	20.24	107.00	1175	3285	2940	166.00	<L.D.
Dy	3.39	2.72	1.72	3.92	1.72	3.92	1.55	2.18	5.81	3.49	3.40	1.61	0.36	0.50	2.86	5.08
Er	1.80	1.48	0.95	2.11	0.95	2.11	0.87	1.18	3.39	1.94	1.87	0.95	0.23	0.29	1.49	4.74
Eu	1.02	0.82	0.80	1.57	0.85	1.21	1.68	1.25	1.16	1.25	1.24	0.58	0.08	0.09	1.29	1.00
Gd	3.79	3.21	1.87	4.62	1.76	2.56	5.84	3.71	3.88	4.26	3.69	1.82	0.33	0.29	3.67	3.37
Hf	1.07	1.05	0.59	1.23	0.59	0.75	1.32	0.90	1.02	1.21	0.89	0.97	0.16	0.18	3.21	6.81
La	0.53	6.53	3.28	7.46	3.58	8.34	7.16	5.19	5.43	4.93	5.26	8.34	0.45	0.24	15.30	5.96
Lu	0.25	0.24	0.13	0.30	0.12	0.17	0.51	0.26	0.29	0.32	0.26	0.16	0.04	0.06	0.24	1.35
Nb	2.00	2.46	0.99	2.45	0.98	1.75	4.74	1.70	1.79	1.82	1.87	1.45	00.13	0.17	3.55	3.13
Nd	15.77	17.82	6.90	18.72	6.71	12.08	20.28	13.79	13.22	15.35	13.65	9.74	0.69	0.58	23.70	10.08
Ni	116.30	127.30	91.49	81.10	29.74	25.74	6.20	7.80	6.58	22.64	45.44	66.20	1229	1234	66.30	<L.D.
Pb	<L.D.	<L.D.	2.24	2.20	2.88	3.79	2.16	2.63	2.62	<L.D.	3.01	8.88	0.47	0.26	4.86	2.11
Pr	3.14	3.90	1.33	3.68	1.33	2.65	3.86	2.62	2.51	2.93	2.61	2.33	0.19	0.12	5.42	2.13
Rb	1.47	1.28	16.84	3.23	32.46	1.07	0.75	0.72	2.14	1.74	2.41	1.78	1.27	0.72	23.30	3.98
Sm	4.14	3.89	1.91	4.94	1.83	2.90	5.61	3.92	3.86	4.35	3.81	2.09	0.20	0.25	4.86	2.72
Sr	90.95	49.10	516.50	559.70	747.50	685.60	524.40	612.70	546.50	294.70	507.10	282.80	13.30	20.50	487.00	396.50
Ta	0.12	0.12	0.07	0.14	0.07	0.13	0.27	0.10	0.12	0.11	0.12	0.10	0.01	0.02	0.30	0.17
Tb	0.57	0.47	0.29	0.67	0.27	0.38	0.92	0.58	0.60	0.67	0.57	0.27	0.05	0.06	0.51	0.66
Th	0.12	0.09	0.15	0.26	0.20	0.87	0.12	0.30	0.38	0.20	0.35	0.92	0.03	0.00	1.37	0.36

Table 1. Contd.

Tm	0.26	0.23	0.14	0.32	0.12	0.17	0.50	0.28	0.31	0.34	0.28	0.14	0.04	0.05	0.22	0.88
U	0.06	0.06	0.08	0.13	0.12	0.41	0.07	0.13	0.14	0.08	0.17	0.35	tr	tr	0.87	0.45
V	231.20	382.40	231.10	240.40	250.20	67.65	189.70	209.10	192.40	547.40	172.50	227.10	62.70	101.00	126.00	6.17
Y	17.53	15.56	9.07	21.06	8.49	11.74	31.90	18.33	19.44	22.30	17.85	9.61	2.66	3.24	15.30	37.38
Yb	1.69	1.46	0.87	1.95	0.78	1.07	3.26	1.76	1.91	2.13	1.74	0.98	0.23	0.35	1.47	7.13
Zr	27.38	25.55	15.14	34.72	18.30	21.31	33.44	23.82	27.90	30.68	23.41	36.34	6.22	6.03	119.00	332.60
Mg#	0.55	0.55	0.46	0.39	0.42	0.33	0.29	0.35	0.35	0.43	0.37	0.57	0.74	0.77	0.44	0.20

Precision of analytical errors is given I the section materials and method, PF= Loss of ignition; LD= detection limits; Metapyrox= metapyroxenite; Grt-A= Garnet-amphibolite, Grt Free A= Gernte-Free6Amphibolite; F Amp= Fine grained amphibolites; Ultrabasic R.= Ultrabasic Rocks; Tonal.= Tonalite; Q-Dio= Quartz-Diorite ; Fe2O3 is recalculated with $Fe^{3+}/(Fe^{3+} + Fe^{2+})=0.05$.

are highlighted on cross-sections (Figure 3).

Petrography

Hand samples of mafic to ultramafic plutonic rocks assemblage include metaultrabasites (serpentines), metapyroxenites, isotropic metagabbros, garnet-amphibolites, quartz- metadiorite and garnet-metatonalites.

Metaultrabasites

The metaultramafic rocks (Th538 = Fpd4, Th738) crop out as small lenticular bodies. Relict of magmatic textures are fine to coarse grained orthocumulate with crystal sizes varying from less than 1 to 3 mm. The cumulus phase is olivine, and clinopyroxene being the main post cumulus phase locally transformed into amphibole. Heteradcumulat texture occurs in some samples with euhedral olivine encompassed by large clinopyroxene crystal 2 to 3 cm sized (Photos 1 and 2, Figure 4). Accessory mineral is spinel ineuhedral to anhedral crystals. Magnesian-chlorite, talc, serpentine, tremolite and calcite occurred as metamorphic minerals.

Metapyroxenites

Metapyroxenites dark gray to blackish in color, coarse-grained (3 to 5 mm), massive rocks locally cut by whitish feldspathic vein lets. They intruded schistose metabasaltes with pillowed, flattened structures (photos 1 and 2, Figure 5).

These rocks show accumulate magmatic texture, with cumulus mineral being the amphibole resulting from retromorphosed pyroxene. Intercumulus phase is represented by a few interstitial crystals of magmatic plagioclase (plagioclase 1), which recrystallized in small-sized plagioclase 2 crystals. Secondary minerals replacing amphibole are zoïsite , sericite , small crystals of secondary quartz , chlorite, and clinozoisite pistachite.

Metagabbros

The metagabbros are massive, coarse-grained (3 to 10 mm), meso- to melanocratic. The leucocratic ones are scarce and poor in ferromagnesian minerals (Fpd5). In thin section, plagioclase is intensely retrograde to epidotes and sericite, amphibole being in turn partially replaced by epidotes and chlorite. They are locally metamorphosed into massive coarse-grained-amphibolites or foliated garnet or garnet-free-amphibolites. In thin sections, textures are grano-nematoblastic to nematoblastic, with metamorphic minerals being hornblende and plagioclase, and accessory minerals are sphene and opaque. Hornblende is partially replaced by epidotes and chlorite. Small secondary quartz crystals and white mica are secondary minerals of plagioclase retrogression. Garnet-amphibolites occur from decimetric to multidecimetric chaotic blocks to decametric to multidecametric panels. Globular garnet (2 to 3 mm) is crystalized in white to reddish, centimetric to multicentimetric feldspathic bands, or aggregated as pockets of grenatites (Photos 1 and 2, Figure 6). These garnet enriched bands and pockets could represent feldspath injections of leucocratic gabbro in mesocratic to melanocratic ones prior to metamorphism. In thin sections, the garnet appears as composite or framboid crystals containing inclusions of plagioclase 1 and amphibole 1 with normal continuous zonation. The magmatic mineral relics

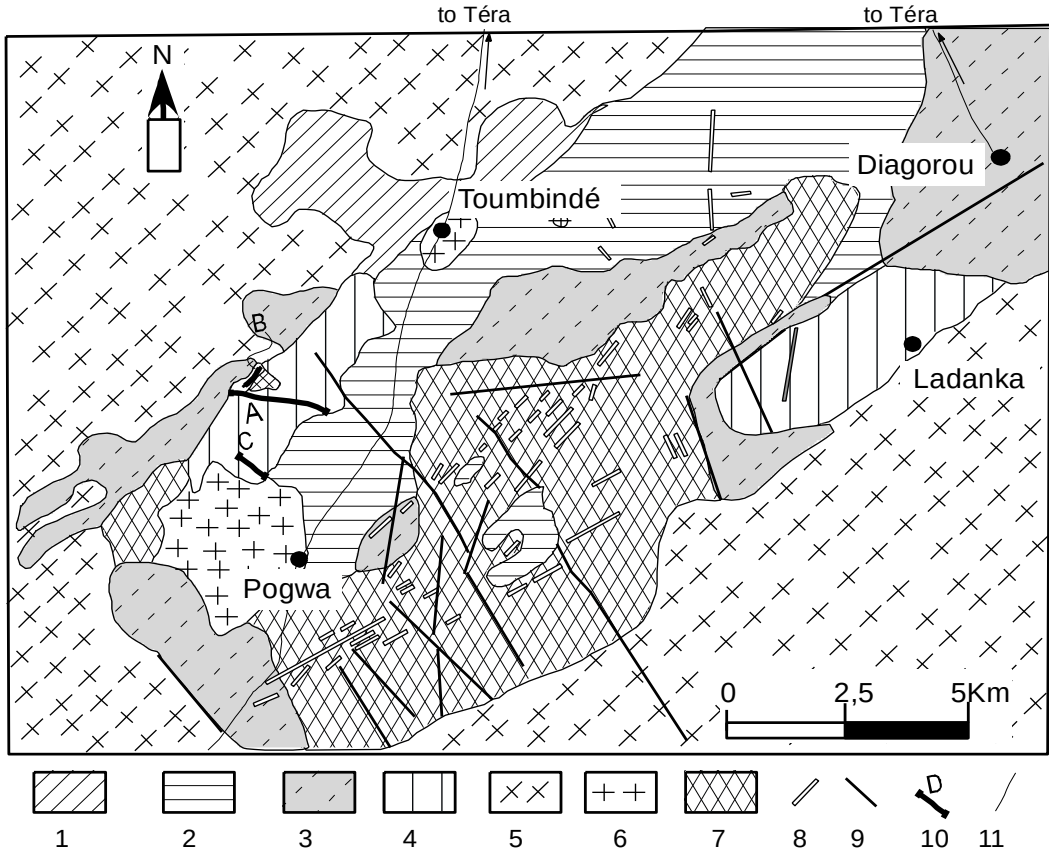

Figure 2. Geological map of Pogwa of and cross section locations. 1. Metbasalts; 2. Talschists; 3. Amphibolits; 4. Basic and ultrabasic plutonic rocks; 5. Granitoids; 6. Late granits; 7. Quartz metadiorite; 8. Dyke of quartz; 9. Fault; 10. Crosssection locations; 11. Tracks.

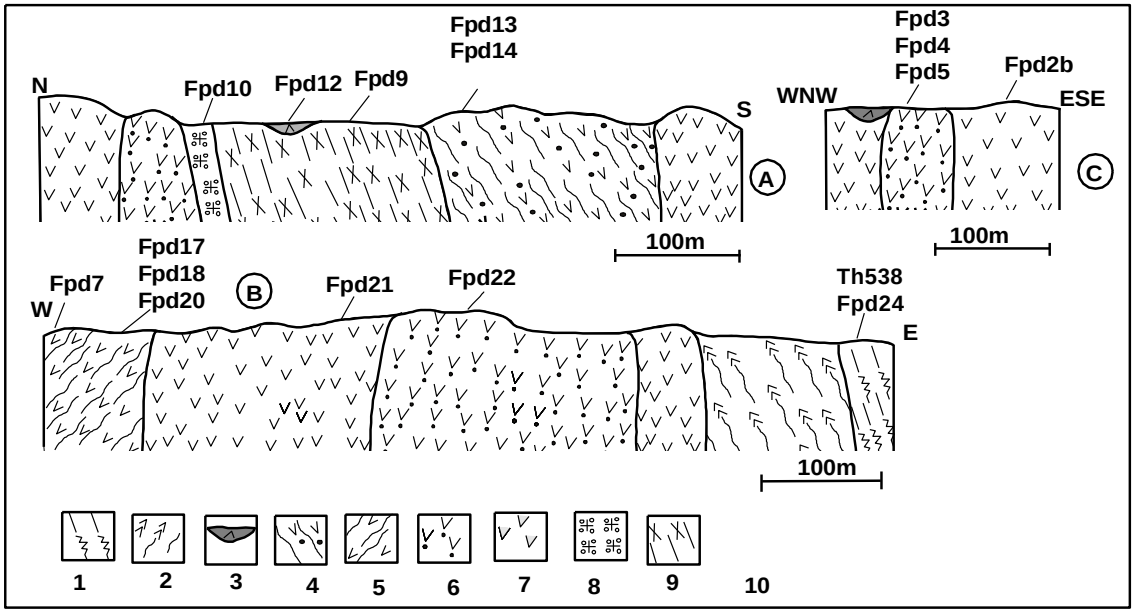

Figure 3. Geological cross-sections and sample locations. 1: Ultrabasic rocks; 2: Talcschists and talc-chloritoschits; 3: Blocks of metabasalts; 4: Garnet-Amphibolite; 5: Amphibolite (metagabbro); 6: Isotropic metapyroxenites; 7: Isotropic metagabbros; 8: Garnet metatonalites; 9: Quartz-metadiorite.

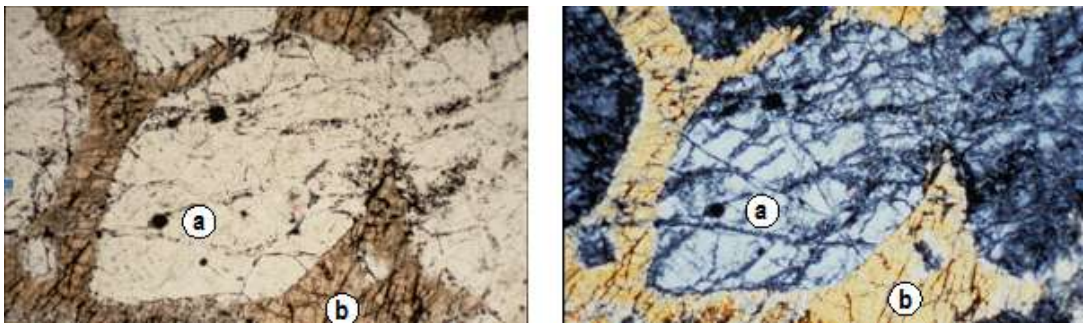

Photo 1 **photo 2**

Figure 4. Relic of magmatic texture in ultrabasic rocks.

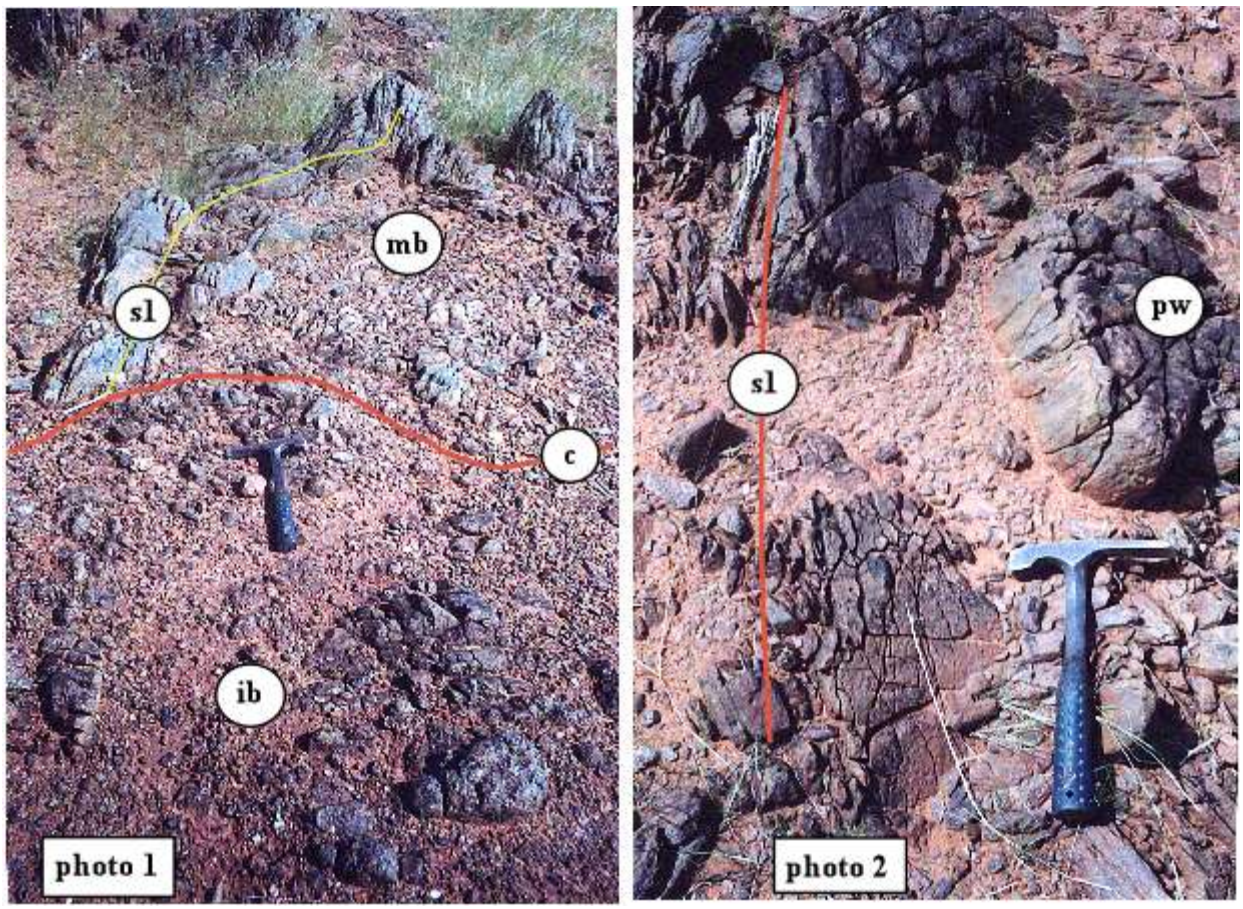

Figure 5. Field diagrams showing pyroxenite intrusive in metabasaltes. Photo 1 : Basic intrusive rock (ib) cross cutting a metabasalte (mb) with schistose structure (s1), and (c) the contact between the rocks. Phot 2 : metabasalts with flattened pillowed and suitcase structure.

(amphibole 1, plagioclase 1),metamorphic minerals (amphibole2 and plagioclase 2) and post-metamorphic ones (retrograde minerals) are the same as described in metgabbros. Retrogression of garnet results in thin layers of chlorite in crystal breaks and edges.

Tonalite and quartz-metadiorite

Tonalite (fpd10) and quartz metadiorite (Fpd9) are coarse-grained texture and have foliated structure emphasized by irregular foliation, sigmoidal around quartz and

Photo 1

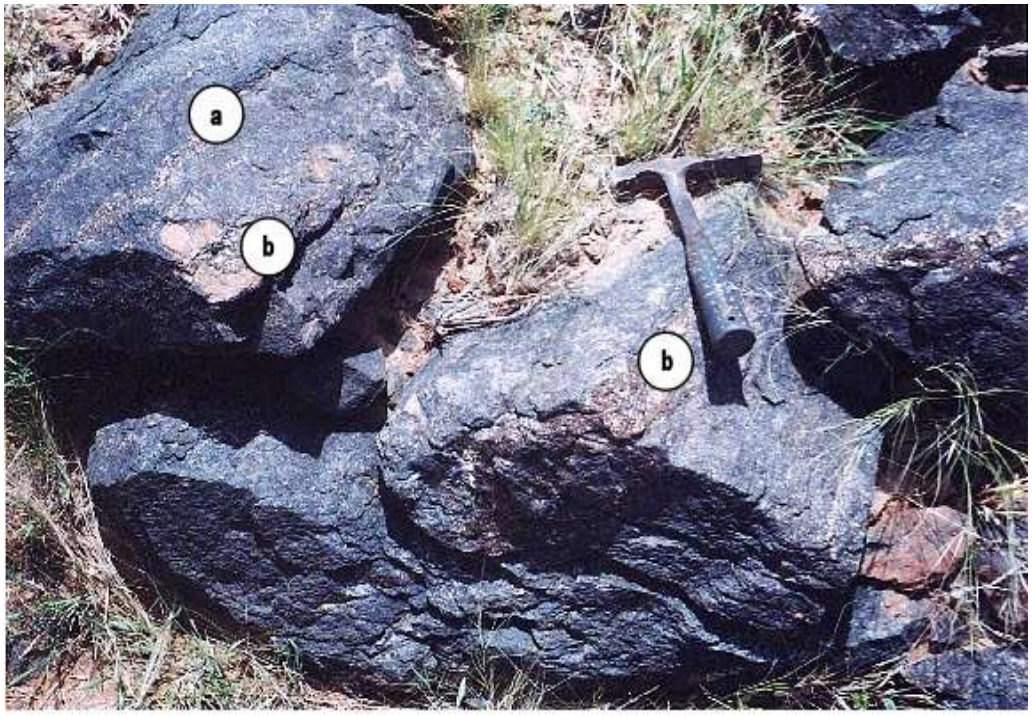

Photo 2

Figure 6. Blocls of granite amphibolite. Photo 1 (a) garnet free amphibolite ; (b) feldspathic bands with garnet ; (c) pockets of garnet (grenatite) ; Phot 2 (b) white feldspaathic garnet bands ; (b) pockets of grenatite.

feldspar. These rocks show decimetric to metric enclaves and panels of metabasaltes, namely fine-grained-amphibolites (Fpd12) cut by quartz veinlets. In thin section, the textures of these rocks are grano-lepido-nematoblastic, with magmatic plagioclase 1 (sub-automorphic to automorphic zoned crystals), biotite,

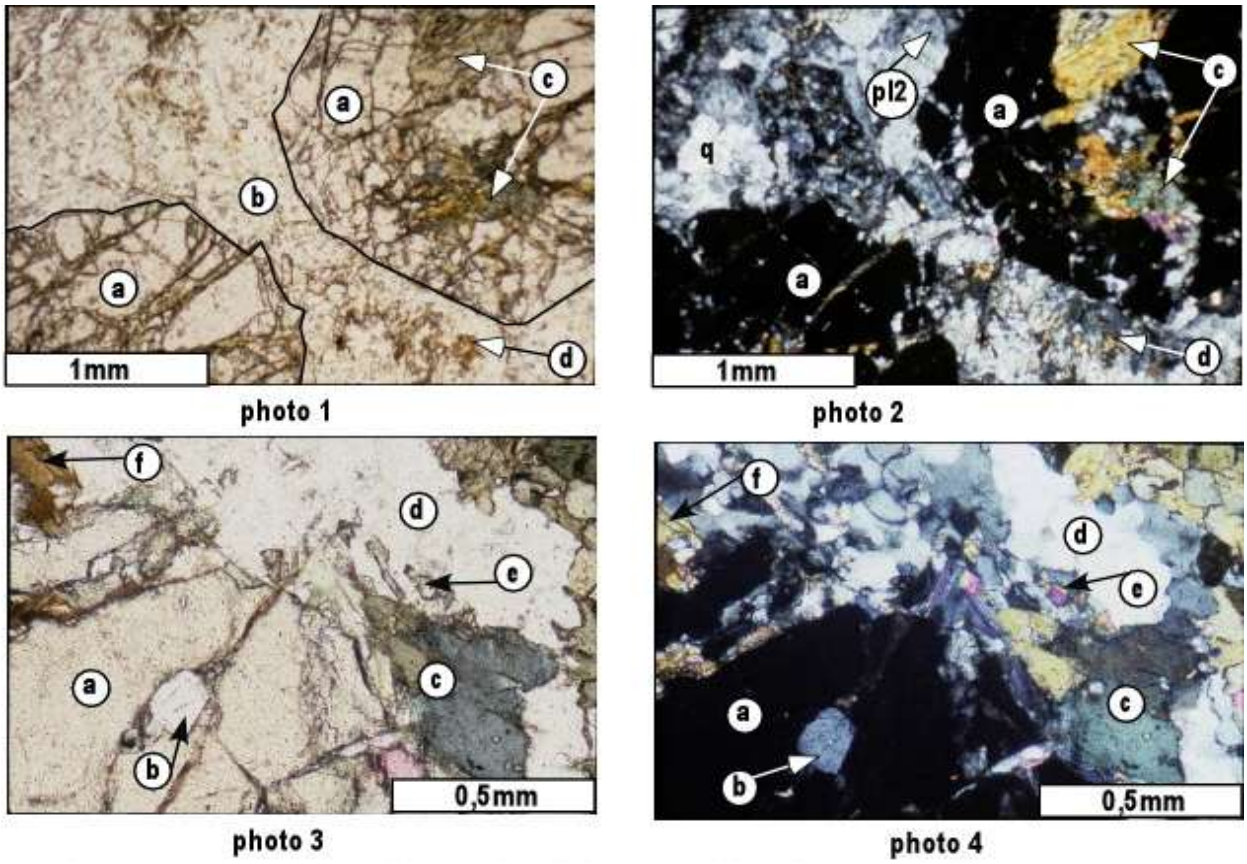

Figure 7. Thin section of quartz-matadiorites. Photos 1 and 3 are observed in NAPL and photos 2 and 4 observed in APL (a) Garnet ; (b) plagioclase ; (c) amphibole 1 under retrogression (d) biotite ; (pl2) plagioclase 2 ; (q) quartz € epidote ; (f) biotite.

hornblende 1 and large quartz crystals. Metamorphic minerals are hornblende 2, smaller quartz crystals, biotite and plagioclase 2, the latter being anheudral. Composite to framboid garnet crystals, with inclusions of plagioclase 1 and amphibole 1 are present in sample Fpd10 (Photos 1 to 4, Figure 7).

Geochemistry

The Pogwa rocks exhibit broad variation of the mg# parameter (mg# = MgO / MgO + FeO). Ultrabasic rocks (Samples 738 and Th538 samples) are characterized by quite high values 0.74 and 0.77. For the other rocks mg# varying from 0.20 to 0.57 may indicate evolved rocks, however, variation in SiO_2 content is not coherent with this evolution. This is emphasized by water content (PF) or loss of ignition. Ultrabasic rocks with 39.63 and 44.46% SiO_2 show the highest content PF (8.40 and 5.31%, respectively) in relation to metamorphism and alteration. It is argued that during metamorphism SiO_2 can be leached so that its content will not be coherent with those of immobile elements. For example, in the present study, fine grained-amphibolite (sample Fpd12) has SiO_2 content of 55.52%, with relatively high Cr content (1175 ppm). Sample Fpd-13 (garnet-amphibolite) exhibits low contents of Cr (9.94 ppm) and Ni (6.20 ppm), with 43.66% of SiO_2. For other samples (except in the case of Fpd-2 and ultrabasic rocks) SiO_2 contents vary from 44.38 to 50.42% while those of Cr are less than 200 ppm. Al_2O_3 contents are low in ultrabasic rocks (1.39 to 6.58%), MgO contents are higher (23.36 to 32.19%), FeO (8.78 and 11.27%). The highest compatible trace elements contents such as Ni (1229 and 1234 ppm) and Cr (2940 and 3285 ppm) are found in ultrabasic rocks, while rare earth elements (REE) contents are low (La = 0.24 and 0.45 ppm; Lu = 0.04 and 0.06 ppm).

Tonalite (Fpd10) and quartz-diorite (Fpd9) are rich in silica with, respectively 68.52 and 60.29% SiO_2. The content of other major elements are $Al_2O_3 \approx 15.55\%$, FeO = 5.62and 4.31%, MgO = 4.48 and 1.07, CaO = 6.76 and 5.79%. The contents Na_2O and K_2O are not discussed because they are very mobile during metamorphism and alteration. This is confirmed by K_2O below limit of detection in many samples. The highly evolved character of sample Fpd10 is emphasized by the contents of compatible trace elements such as Cr and Ni below the detection limit (L.D), whereas hygromagmatophiles

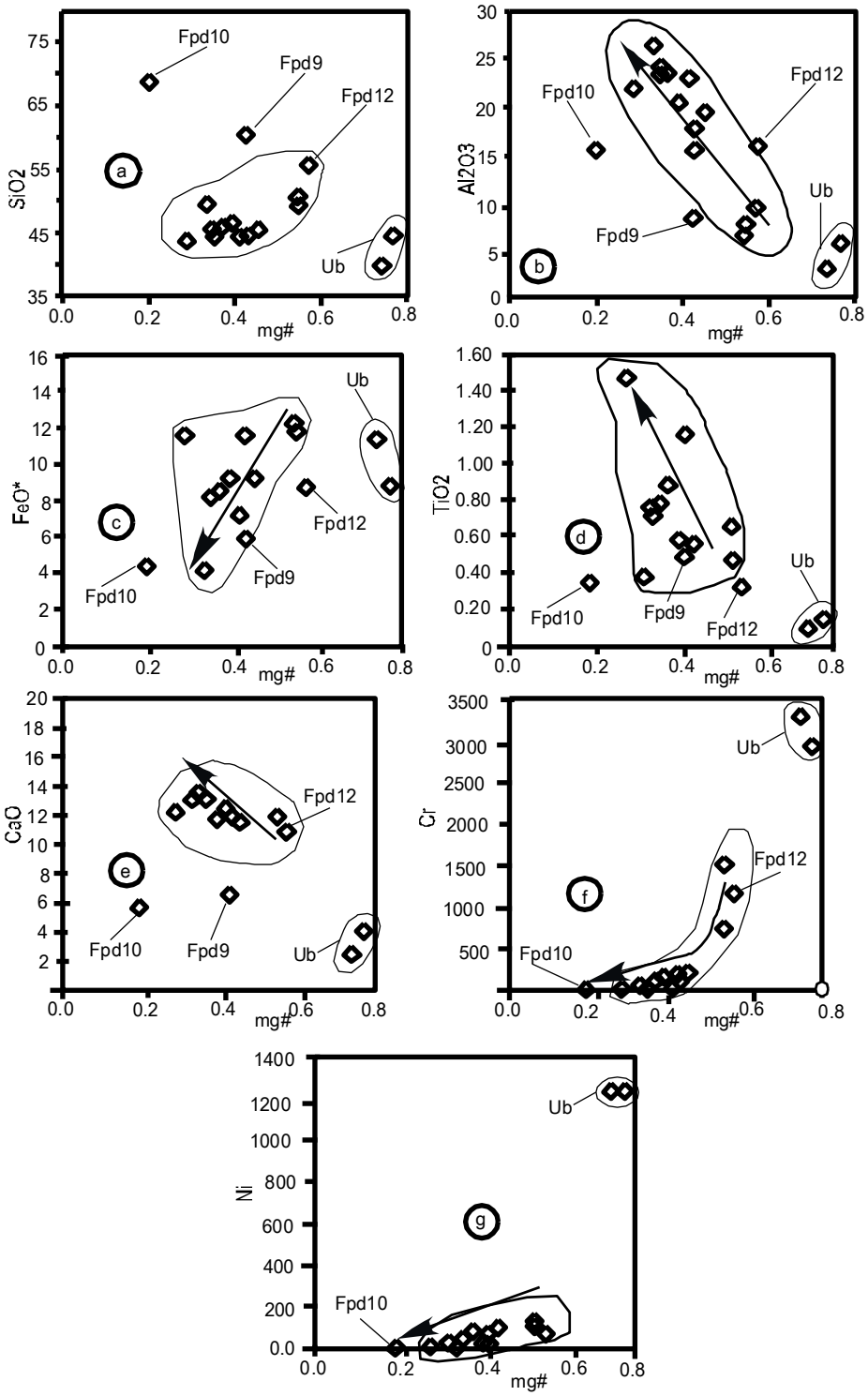

Figure 8. Harker diagrams for major and trace elements versus mg#

elements, such as Hf and Zr are enriched with 6.81 and 3.21 ppm, 332 and 119 ppm, respectively. The LREE are rather enriched (La = 5.69 and 15.30 ppm; Ce = 14 and 37.10 ppm) compared to HREE (Lu =0.24 and 1.35; Yb = 1.47 and 7.13 ppm).

Harker diagrams for major elements (oxides vs mg#) and traces elements (Ni and Cr vs mg#) are given in Figure 8.

All diagrams show the composition gap between metaultrabasic rocks and metagabbroic rocks. Samples

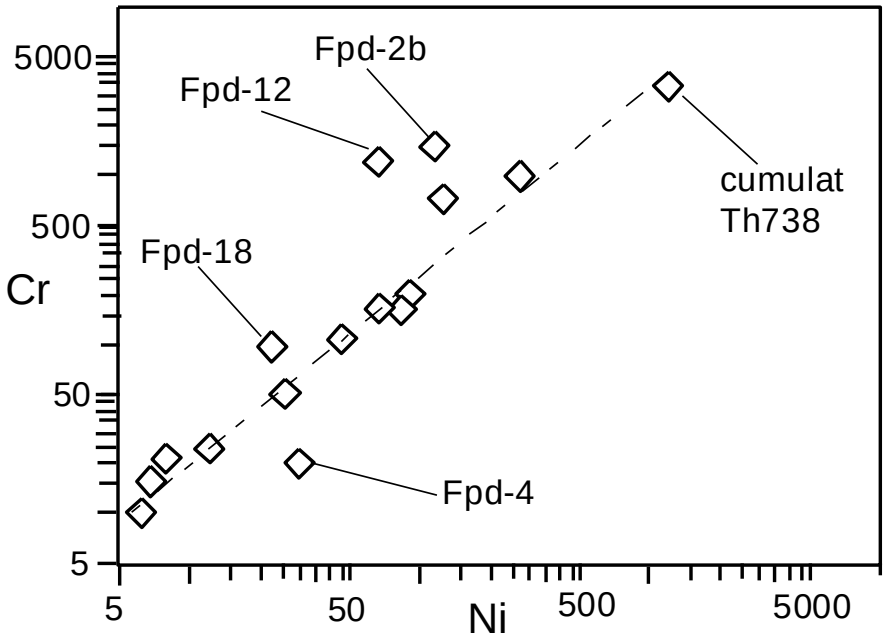

Figure 9. Diagram log(Cr) = f(log(Ni) for gabbroic rocks of pogwa.

are scattered in mg#-SiO_2 diagram, with no significant trend (Figure 8a). mg#-Al_2O_3 diagram (figure 8b) shows some trend which is suggestive of fractional crystallization of ferro-magnesian minerals (pyroxene-olivine) in magmatic chamber. Weak variation trend in FeO* (figure 8c) is in accordance with ferro-magnesian fractionation. TiO_2 exhibits light enrichment with evolution trend (Figure 8d), this is consistent with non-fraction of Ti-oxide phases. Spinel, olivine and pyroxene crystallization is suggested by decreasing trends of Cr and Ni in diagram Cr vs Mg# (Figure 8f) and Ni vs Mg# (Figure 8g).

The diagram log(Cr) = f(log(Ni)) reveals a good trend in Cr and Ni variation within Pogwa rocks (Figure 9) except for fine grained amphibolite (Fpd-12) and meta-pyroxenites (Fpd-2b and Fpd-18). It means that fractional crystallization of pyroxene and olivine had played important role in the genesis of these rocks. But the variable partial melting degrees could explain Cr and Ni contents in samples Fpd-12, Fpd-2b and Fpd-18.

The chondrite C1 normalized REE patterns (Taylor and McLennan, 1985) for gabbroic rocks and ultrabasic rocks, quartz-diorite, tonalite and fine-grained amphibolite are reported in Figures10a and b, respectively. Gabbroic rocks of Pogwa are enriched in Light REE (LREE) with La_N/Yb_N ranging from 1.45 to 5.19, and parallel patterns suggest fractional crystallization. This is evidenced by Eu anomalies. Indeed Eu* = $2EuN/(Sm_N+Gd_N)$ with positive anomalies (Eu* = 1.29 to 1.43) and negative ones (0.77 to 0.91) is indicative of plagioclase fractionation. Ultrabasic rocks show relatively flat (sample Th738) to slightly LREE enrichment pattern (sample Th538), with Eu* = 0.43 and 1.05, respectively.

Quartz-diorite (Fpd10) and fine grained amphibolite (Fpd12) have parallel patterns, and are LRRE enriched with La_N/Yb_N = 6.7 and 5.53, respectively. The trend of patterns suggested that these rocks are generated from the same source by fractional crystallization of ferro-magnesian minerals and few plagioclase as enhanced by light Eu negative anomalies (Eu* = 0.90). The tonalite sample (Fpd10) is distinctively different from the other rocks with Heavy REE (HREE) enrichment (La_N/Yb_N = 0.46). This rock may be generated by partial melting of HREE enriched source, more particularly garnet bearing residue.

Spider diagrams (normalized to MORB-N, Bevins et al., 1984) are shown in Figures10a and b. Most of the gabbroic rocks are enriched in large ion lithophile elements (LILE: Sr, Rb, Ba, K) and LREE, but depleted in HREE relative to the MORB (Figure 10b). Negative anomalies in Nb, Ta; Zr, Hf and Ti are indicative of high field strength element (HFSE) depletion. Ultrabasic rocks exhibit two patterns. The pattern of sample Th738 is similar to those of gabbroic rocks, with relatively LILE, LREE enrichment and light HFSE depletion. The pattern of Sample Th530, with light Ta and HREE enrichment, is not similar to those of gabbroic rocks.

Patterns of quartz-diorite and fine grained amphibolite have similar features with the gabbroic rocks, such as enrichment in LILE and depletion in HREE and HFSE (Figure 10b). It is assumed that these rocks were generated dominantly by crystal fractionation, with minor crustal contamination suggested by LILE enrichment. The tonalite (sample Fpd10) is characterized by low depletion in Nb, Ta, LREE and relative HFSE and HREE enrichment.

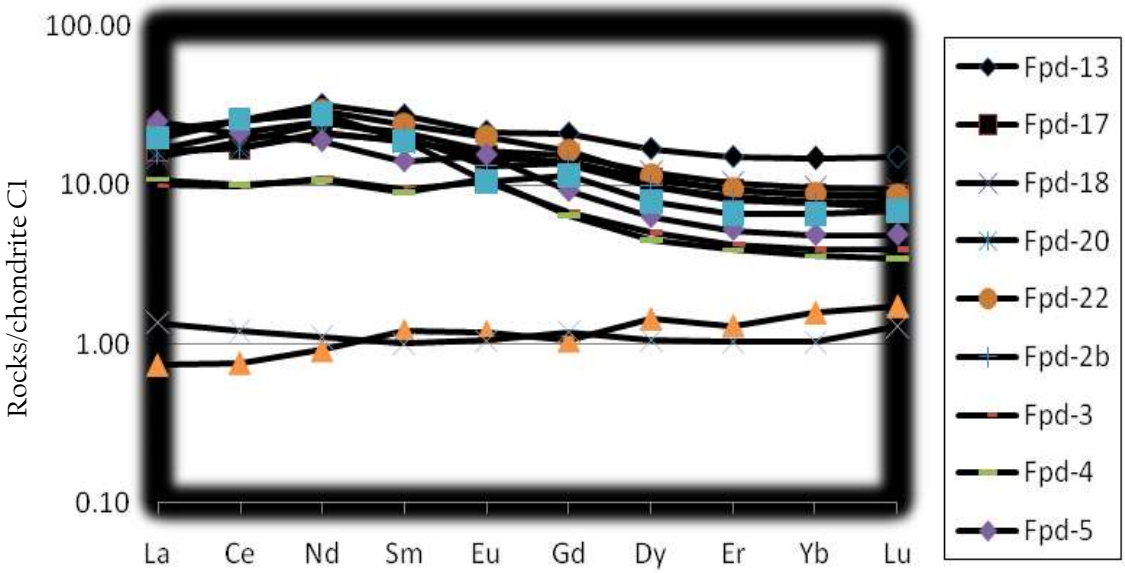

Figure 10a. REE abundances of gabbroic rocks and ultrabasic rocks normalized to C1 chondrite.

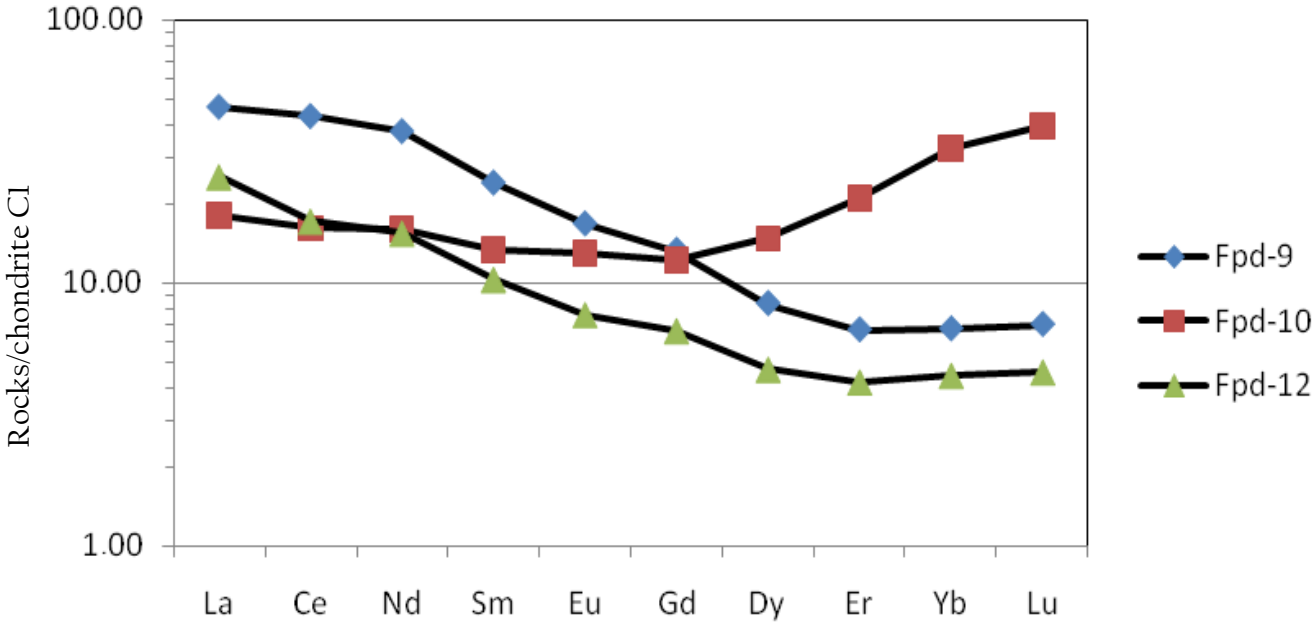

Figure 10b. REE abundances of other rocks normalized to C1 chondrite

In Zr-Nb-Y discrimination diagrams of Figure 11 (Meschede, 1987, Pearce, 1982, 1884), gabbroic rocks plot within plate tholeiites and volcanic-arc basalts field (C), and in N-MORB and volcanic-arc basalts field (D) (Figure 11). Figure 12 (Y-Cr) clearly shows that the gabbroic rocks of Pogwa have good affinities with arc-volcanic basalts. They are genetically linked and regarded as arc-related plutonic rocks.

DISCUSSION

Ultrabasic and basic plutonic rock assemblage of North Pogwa is made up of serpentinite, pyroxenites gabbroic rocks, fine grained-amphibolite, quartz-diorite and tonalite. These rocks are metamorphosed into greenschist to amphibolite facies as corroborated by H_2O content (PF = loss of ignition) varying from 0.08 to 8.40%. The behavior

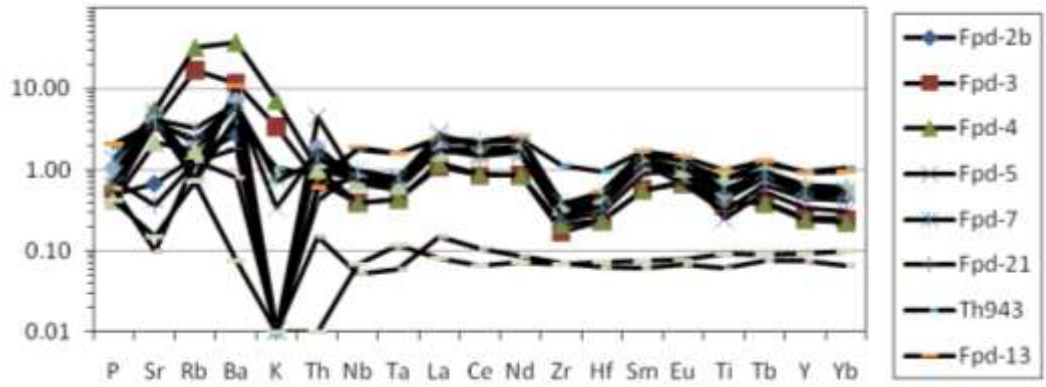

Figure 10c. Spider diagram gabbroic rocks and ultrabasic rocks normalized to N-MORB.

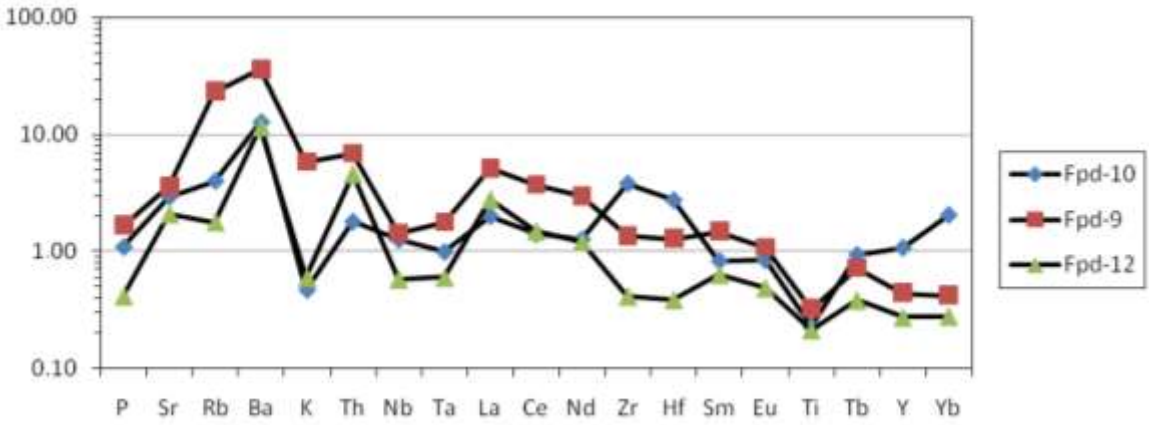

Figure 10d. Spider diagram of others rocks normalized to N-MORB.

of some major elements such as SiO_2, Na_2O, K_2O and CaO are influenced by metamorphism so that, they are not correlated with immobile compatible elements, particularly Cr and Ni. These elements show a good trend that emphasized the role of crystal fractionation in the geneses of many of these rocks. Variation of Cr contents in some samples (Fpd2b, Fpd-12 and Fpd18; figure 9) may be related to variable partial melting degrees. Exception for samples Th538 and Fdp-9, all samples are characterized by:

- REE normalized to C1 chondrite patterns enriched in LREE and depleted in HREE. The abundances of these elements increase with differentiation.
- Variable Eu* anomalies are indicative of plagioclase fractionation;
- N-MORB normalized spider diagram patterns show LILE and LREE enrichment combined with Nb-Ta and HFSE anomalies.

In Y-Cr discrimination diagram, samples are plot in arc-magmatic environment (Figure 12). Quartz-diorite and fine grained-amphibolite, despite the afore mentioned characters, seem to have mantellic source which is different from that of gabbroic rocks. These features characterize subduction related magma generated by partial melting of metasomatised mantle wedge, with LILE enrichment. These elements may be transported from subducting slab to the mantle wedge by dehydration fluids. The HFSE depletion corroborated by negative anomalies in spider gram is linked to the stability of phaseminerals partitioning them during metasomatism and partial melting.

Sample Th538 has REE pattern with depletion in LREE relatively to HREE. Multi-elements pattern is relatively flat, similar to MORB-N, with absolute depletion in all trace elements. The sample is considered to be serpentinised cumulate rocks coming from the basic pile representing paleaoproterozoic oceanic crust extensively studied in the West African craton (Abouchami et al., 1990; Boher et al., 1992; Lompo, 2009). This is corroborated by field relations and cross sections of

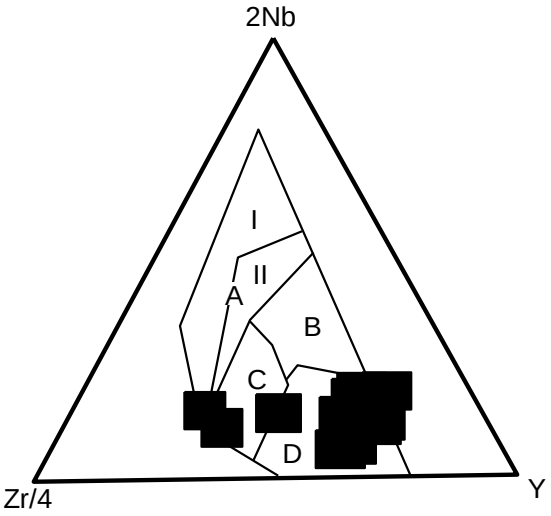

Figure 11. Zr-Nb-Y discrimination diagram for Pogwa rocks AI, within plate alkali basalts ; AII, within plate and alkali and within plate tholeiite ; B, E-MORB ; C, within plate tholeiites and volcanic-arc basalts ; D, N-MORB and volcanic-arc basalts (samples reported = gabbroic rocks, fine grained amphiobolite and quartz-diorite).

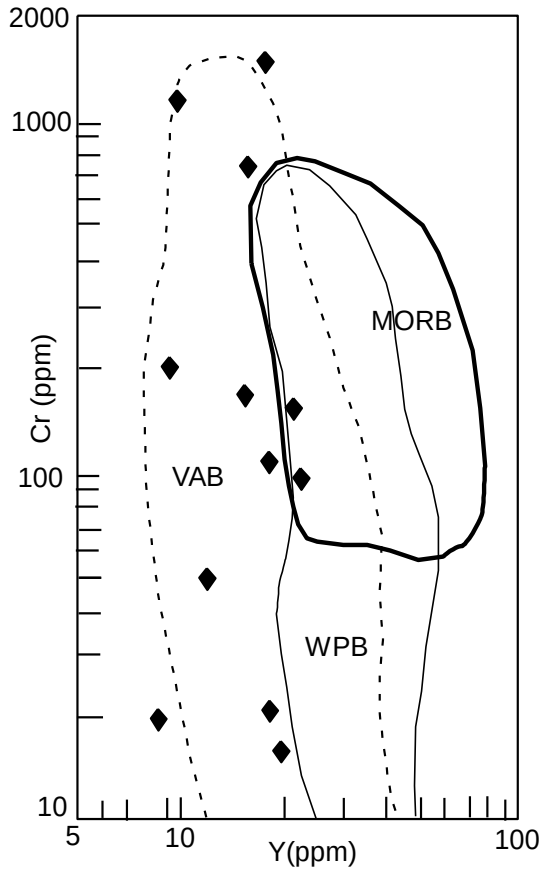

Figure 12. Cr-Y discrimination daigram (Pearce, 1982). VAB = volcanic-arc basalts ; WPB = within plate basalts, MORB = middle oceanic ridge basalts

Figure 3. The REE pattern of the tonalite (sample Fpd10) shows a significant enrichment in HREE compared to LREE. In discrimination diagram Rb-(Y+Nb) of Prearce (1984), sample Fpd10, with Rb = 3.98 ppm and (Y+Nb) = 40.51 ppm, plots in the field of Oceanic rigde granite (ORG) resulting from ultimate crystal fractionation of depleted magmatic liquid. In the present study, the tonalite (sample Fpd-10) is considered as final product of fractional crystallization that generated paleoproterozoic oceanic crust. The mantle source of this oceanic crust may be enriched in HREE, suggesting garnet-free residue. The afore mentioned features demonstrated that, Pogwa ultrabasic-basic plutonic rocks witness a root of a paleoproterozoic oceanic-arc.

In West Africa, such geodynamic environment is under debate. However, many geochemical results from birimian rocks supported the presence of subduction zones (for example, Beziatet al., 2000). Furthermore, recent metamorphic studies in Burkina Faso, West Africa (Ganne et al., 2012) pointed out geothermal gradient of 10 to 12°C/km similar to those of modern subduction zones in West African Craton.

Conflict of Interests

The authors have not declared any conflict of interests.

ACKNOWLEDGEMENTS

The authors are grateful to, and acknowledge the efforts of, the reviewers for their observations which have greatly improved the manuscript.

REFERENCES

Abouchami W, Boher M, Michard A, Albarède F(1990). A Major 2.1Ga event of mafic magmatism in West Africa: An early stade of crustal accretion, J. Geophys. Res. 95:17605-17629.

Ama-Salah I, Liegeois JP, Pouclet A(1996). Evolution d'un arc insulaire océanique birimien précoce au Liptako nigérien (Sirba) : géologie, géochronologie et géochimie, J. Afr. Earth Sci. 22:235-254.

Bevins RE, Kokelaar BP, Dunkley PN (1984). Petrology and geochemistry of early to mid-Ordovician Igneous rocks in Wales: a volcanic arc to marginal basin transition, Proc. Geol. Assoc 95:337-347.

Beziat D, Bourges F, Debat P, Lompo M, Matrin F, Tollon F (2000). A Paleoproterozoicultramafic-mafic assemblage and associated volcanic rocks of the Boromo greenstone belt: fractionates originating from island-arc volcanic activities in the West African craton, Precambrian Res. 191:25-47.

Boher M, Abouchami W, Michard A., Albarede F, Arndt NT (1992). Crustal growth in West Africa at 2.l Ga. J. Geophys.Res. 97:345-369.

Cheilletz A, Barbey P, Lama C, Pons J, Zimmerman J-L, Dautel D (1994). Age de refroidissement de la croûte juvénile birimienne d'Afrique de l'Ouest, Données U/Pb et K-Ar sur les formations à 2.1Ga du SW du Niger, C. R. Acad. Sci. Paris II(319):435-442.

Dupuis D, Pons J, Prost A E(1991). Mise en place des plutons et caractérisation de la déformation birimienne au Niger occidental, C. R. Acad. Sci Paris 312:769-773.

Gasquet D, Barbey P, Adu M, Paquette JL (2003). Structure, Sr–Nd

isotope geochemistry and zircon U–Pb geochronology of the granitoids of the Dabakala area (Côte d'Ivoire): evidence for a 2.3 Ga crustal growth event in the Palaeoproterozoic of West Africa, Precambrian Res. 127:329-354.
Lahondère D, Thiéblemont D, Tegyey M, Guerrot C, Diabate B (2002). First evidence of early Birimian (2.21 Ga) volcanic activity in Upper Guinea: the volcanics and associated rocks of the Niani suite. J. Afr. Earth Sci. 35:417-432.
Lompo M (2009). Geodynamic evolution of the 2.25-2.0 GaPalaeoproterozoic, magmatic rocks in the Man-Leo Shield of the West African Craton: A model of subsidence of an oceanic plateau,Geological Society, London, Spec. Publications 323:231-254.
Machens E (1973). Contribution à l'étude des formations du socle cristallin et de la couverture sédimentaire de l'Ouest de la République du Niger, Mem. du Bur. Rech. Géol. Minières France 82:167.
Meschede M (1987). Amethod of discrimination between different types of mid-ocean ridge basalts and continental tholeiites with Nb-Zr-Y diagram, Chem. Geol. 56:207-218.
Ganne J, Andrade De V, Weinberg RF, Vidal O, Dubacq B, Kagambega N, Naba S, Baratoux L, Jessell M, Allibon J (2012). Modern-style plate subduction preserved in the Palaeoproterozoic West African craton, Nat. Geosci. 5:60-65.
Pearce JA (1982). Trace element characteristics of lavas from destructive plate boundaries, In Andesites, Edited by Thorpe RS, John Wiley, New York 525-548.
Pearce JA, Harris NB, Tindle AG (1984). Trace element discrimination diagrams for tectonic interpretations of granitic rocks, J. Petrol. 25:956-983.
Pons J, Barbey P, Dupuis D, Leger JM (1995). Mechanisms of pluton emplacement and structural evolution of a 2.1 Ga juvenile continental crust: the Birimian of southwestern Niger, Precambrian Res. 70:281-301.
Pouclet A, Vidal M, Delor C, Siméon Y, Alric G (1996). Le volcanisme du NE de la Côte d'Ivoire mise en évidence de 2 phases de volcanisme distincts dans l'évolution géodynamique du Paléoprotérozoïque, Bull. Soc. Géol. France 167:529-541.
Soumaila A, Garba Z (2006). Le métamorphisme des formations de la ceinture de roches vertes birimienne (Paléoprotérozoïque) de Diagorou-Darbani (Liptako, Niger, Afrique de l'Ouest), Afr. Geosci. Rev. 13(1):107-128.
Soumaila A, Henry P, Garba Z, Rossi M (2008). REE Patterns, Nd-Sm and U-Pb ages of the metamorphic rocks of the Diagorou-Darbani greenstone belt (Liptako, SW Niger): implication for Birimian (Palaeoproterozoic) crustal genesis, Geological Society, London, Spec. Publications 297:19-32.
Soumaila A, Henry P, Rossy R (2004). Contexte de mise en place des roches basiques de la ceinture de roches vertes birimienne de Diagorou-Darbani (Liptako, Niger, Afrique de l'Ouest) : plateau océanique ou environnement d'arc/bassin arrière-arc océanique, C. R. Geosci. 336:1137-1147.
Taylor SR, McLennan SM (1985). The continental crust: its composition and evolution, Blackwell, Oxford 312 p.